JOURNAL OF MATERIALS SCIENCE 31 (1996) 2859–2864

Study on the solidification cracking behaviour of high strength aluminum alloy welds: Effects of alloying elements and solidification behaviours

HWAN TAE KIM, SOO WOO NAM*, SUN HYO HWANG
*Korea Institute of Machinery and Metals P.O Box 101, Yusong, Daejon, 305–600, Korea and *Department of Materials Science and Engineering, Korea Advanced Institute of Science and Technology 373-1, Kusong Dong, Yusong Gu, Daejon, 305–701, Korea*

The solidification cracking susceptibility of the 7000 series Al–Zn–Mg high strength aluminum alloy has been studied. The cracking behaviour of the specimens were evaluated by a Tig–a–Ma–Jig Varestraint test process under various augmented strain conditions. It has been experimentally observed that the addition of copper decreased the solidification cracking resistivity of the high strength aluminum alloy weld metal by increasing the total crack length (TCL). The effect of the addition of manganese on the solidification cracking behaviour is found to be beneficial by markedly decreasing the solidification cracking susceptibility as the manganese content increases from 0.3 to 0.7%. This enhancement by manganese is understood to be attributed to the reduction of the mushy zone size during the solidification process. The effects of chromium and zirconium additions are also investigated. The weld metal containing zirconium is less sensitive to the solidification cracking than the weld metal containing chromium. In addition, the solidification behaviours of the tested alloys are also investigated and it is found that as the solidification temperature range (ΔT) becomes narrow, the solidified structure becomes more dendritic in its features which is believed to create higher solidification cracking resistance.

1. Introduction

Recently, high strength aluminum alloys have been developed by the addition of transition metal alloying elements such as Mn, Cr and Zr. It is well known that small amounts of the transition metal alloying elements added to 7000 alloys play an interesting role in determining fracture toughness, recrystallization and grain refinement [1]. Amongst the transition metal alloying elements Zr is reported to form Al_3Zr particles [2], Cr forms an E-phase [$Al_{18}Mg_2Cr_3$] which displays an incoherent relationship with the matrix and increases the noncrystalline structure and yield strength [3]. In the case of Mn, which is known to form an incoherent dispersoid, it increases the strength and the low cycle fatigue life of the 7000 alloys [4] and additionally shows excellent weldability [5].

It has been reported that a solidification crack occurs between primary dendritic crystals during the solidification of liquified weld metal, and it is one of four types of defects frequently found in the welds of aluminum alloys. These defects include porosity or inclusions, lack of fusion and penetration, and softening in the HAZ [6] which has not melted but heated up to equilibrium solidus of the base material and whose mechanical properties or microstructure have been altered by the heat of welding. There are many reports of the prevention of solidification cracking in the aluminum alloys through the addition of elements such as Ti, B and Zr [7–9]. On the other hand, there have been few reports concerning the effect of addition of Mn and Cr on the solidification cracking behaviour in the welding of an Al–Zn–Mg alloy [10]. The purpose of this study is to investigate the effects of the addition transition metal alloying elements including Mn, Cr and Zr, on the solidification process and on the solidification cracking behaviour of the 7000 series Al–Zn–Mg alloy welds.

2. Experimental procedure

2.1. Materials

The compositions of the aluminum alloys tested are listed in Table 1. The commercial alloys; A (Al 7020), B (Al 7075), and C (Al 7017) and, the recently patented alloy D (Mn containing weldable high strength alloy) [11] were obtained. In addition in order to see the effect of the alloying elements and the solidification process more systematically, the laboratory alloys #1–5 were prepared by melting 99.99 % pure aluminum with the appropriate master alloys and casting in an inert atmosphere. The ingots were homogenized by

0022–2461

TABLE I Chemical composition (wt %) and the solidification temperature range (ΔT) (°C) of the experimental alloys.

No.	Zn	Mg	Cu	Mn	Cr	Zr	ΔT
A	3.96	1.09	–	0.09	0.22	0.16	37.6
B	4.30	2.95	0.48	0.19	0.15	–	40.2
C	4.75	2.40	–	0.32	0.16	0.16	36.0
D	4.15	2.78	–	0.68	–	0.16	33.1
1	4.22	2.64	–	0.72	–	0.12	32.6
2	4.25	2.57	–	0.98	–	0.26	36.5
3	3.82	2.38	–	0.70	0.10	0.29	35.0
4	4.58	2.95	–	0.73	0.24	0.22	38.1
5	4.49	2.69	–	0.75	–	–	37.2

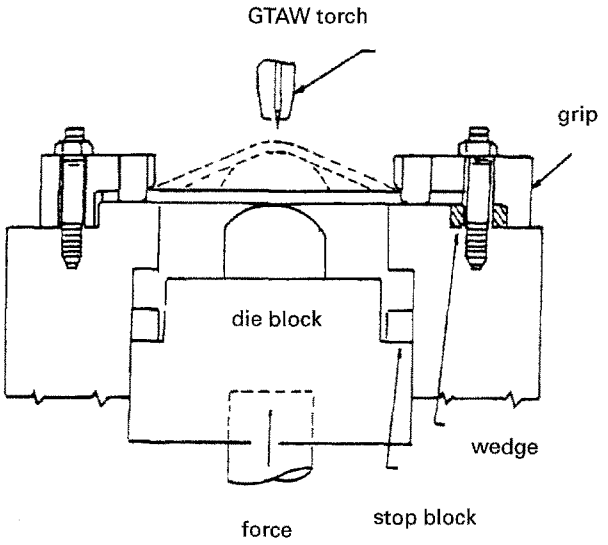

Figure 1 Schematic drawing of the Tig–a–Ma–Jig Varestraint test machine.

TABLE II Welding Parameters.

Current	80–100 A, AC
Voltage	10–12 V
Speed	20 IPM
Shielding Gas	Ar, 30 CFH
Electrode	2% Th, Tungsten
Augmented Strain	1.0–6.0%

heating for 24 h at 460 °C and extruded at 395 °C to make a bar of 28 mm (thickness) × 52 mm (width) with an extrusion ratio of 11.4. The extruded alloys were heated at 460 °C for 90 min followed by water quenching. These bars were naturally aged at room temperature for 96 h and further aged in a two-step process at 100 °C for 10 min and then 160 °C for 180 min.

2.2. Solidification cracking test

The Varestraint solidification cracking tests were conducted on a modified subscale moving torch Tig–A–Ma–Jig type testing system shown in Fig. 1 (Model LT 1100 Serial 9102) which possesses an enhanced capability as compared to the conventional spot Varestraint test apparatus [12]. The specimens were machined to be plates of 12.7 cm length, 2.54 cm width and 3.2 mm depth, and the test conditions of welding are listed in Table II. During a test, an actual weld bead was deposited to simulate the same thermal conditions experienced in an actual welding. Therefore, the microstructures of the tested samples were virtually identical to those encountered in an actual weld. Mechanical restraint was simulated by an externally applied augmented strain.

2.3. DSC test

For the analysis and observation of the solidification process of the liquid weld metal during the gas tungsten arc welding (GTAW), DSC (differential scanning calorimetry, Shimazu TA-50) was used with a scanning rate of 5 °C min^{-1}, and the liquidus and the solidus temperatures of the weld metal were measured.

3. Experimental results

3.1. Solidification cracking behaviour

The susceptibility to solidification cracking of the manganese containing high strength aluminum alloy was compared with that of the commercial Al–Zn–Mg alloys and the results are shown in Fig. 2. Alloy D shows lower solidification cracking susceptibility as compared to the alloys of A, B and C across the whole strain range. Alloy B shows the highest solidification cracking susceptibility at the high augmented strain level of 6.0 %. The threshold strain of alloys A and C is

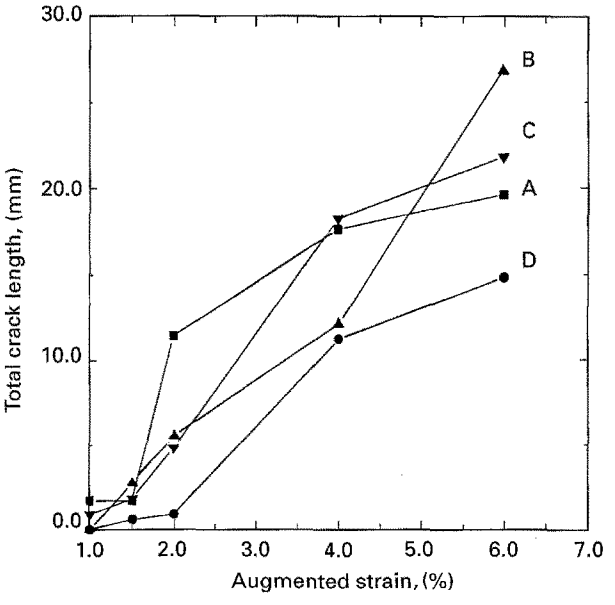

Figure 2 Solidification cracking behaviour of the commercial alloys.

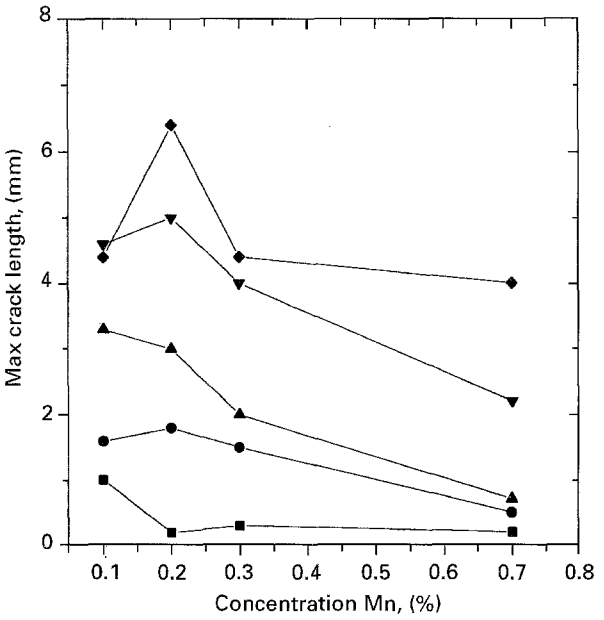

Figure 3 Effect of Mn on the solidification cracking behaviour of the commercial alloy for the various strain. (–■–) ε = 1.0%, (–●–) ε = 1.5%, (–▲–) ε = 2.0%, (–▼–) ε = 4.0% (–◆–) ε = 6.0%.

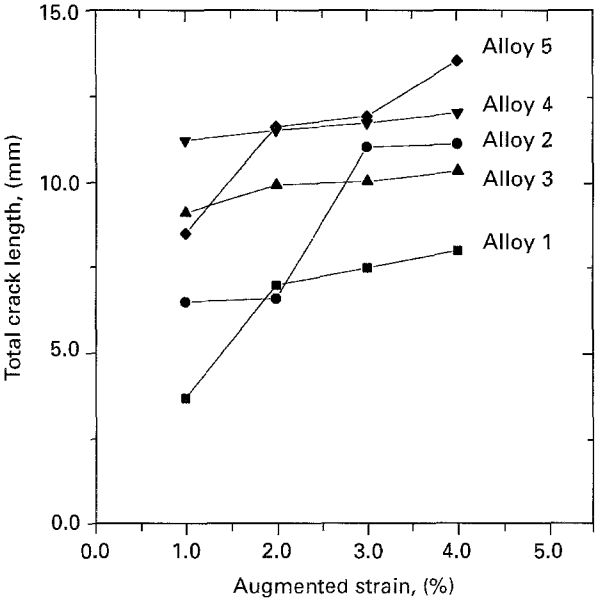

Figure 4 Solidification cracking behaviour of the laboratory alloys.

lower than the other alloys. It is found that additions of Mn gives a beneficial effect, whereas Cu gives a detrimental effect on the solidification cracking resistivity for the Al–Zn–Mg alloys. The effect of the Mn on the solidification cracking behaviour of these alloys is compared in Fig. 3 to indicate that the solidification cracking susceptibility decreases with increasing Mn content when the augmented strain level is low. It also reveals that the solidification cracking susceptibility reaches its peak value at a Mn content of 0.1–0.2 % and then decreases gradually with increasing Mn content up to the augmented strain level of 4.0 %. Fig. 4 shows the total crack length (TCL) of solidification cracking versus augmented strain for the laboratory alloys prepared for this investigation. Alloy 1 shows the lowest solidification cracking tendency compared with the other laboratory alloys. It reveals that the TCL of the Cr bearing alloys, 3 and 4, are large, and the TCL of the 0.98 % Mn alloy 2 and Zr free alloy 5 increase as the augmented strain increases. The optimum amount of Mn in order to have high resistivity to the solidification cracking is found to be 0.72 %. Beyond this optimum level for instance if the Mn content reaches 1.0 %, the solidification cracking susceptibility is observed to increase. It can be noted that these results show the important role of Mn, Cr and Zr during the solidification cracking formation stage. Also that the weld metal solidification cracking behaviour is strongly connected with the solute concentration, solute redistribution, and constitutional supercooling during the weld metal solidification stage as well as the solidified microstructure [13].

3.2. Metallographic and DSC analysis

Metallographic examination was carried out on the laboratory alloy specimens after the Varestraint test. The typical appearance of a solidification cracking feature in this investigation is shown in Fig. 5 for the alloy B which shows the highest solidification cracking susceptibility at an augmented strain level of 6.0%. It is clearly observed that the solidification cracking occurs in the mode of an intergranular and/or interdendritic cracking along the crack sensitive grain It is clearly observed that the solidification cracking

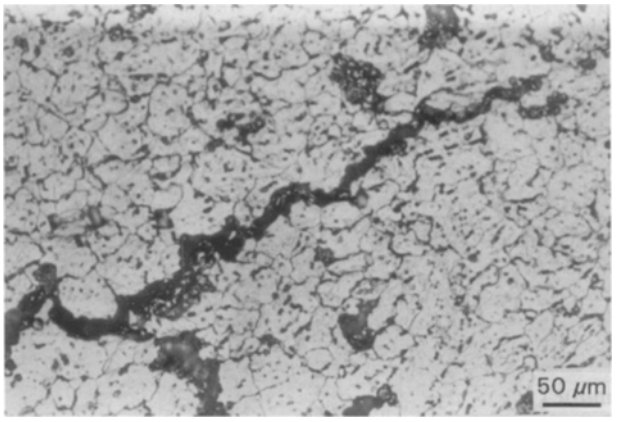

Figure 5 Typical morphology of solidification cracking feature in Varestraint test (alloy B).

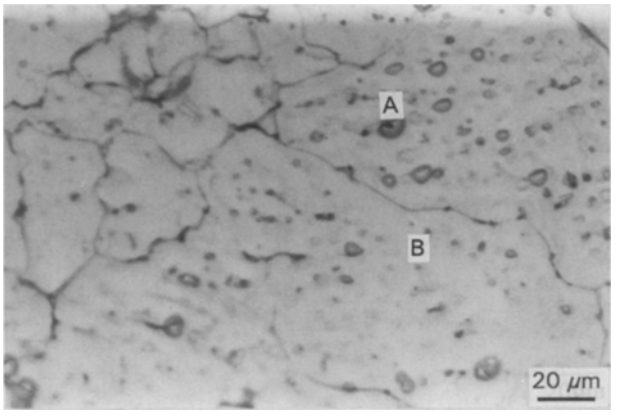

Figure 6 Optical Microstructure of weld metal (alloy 1).

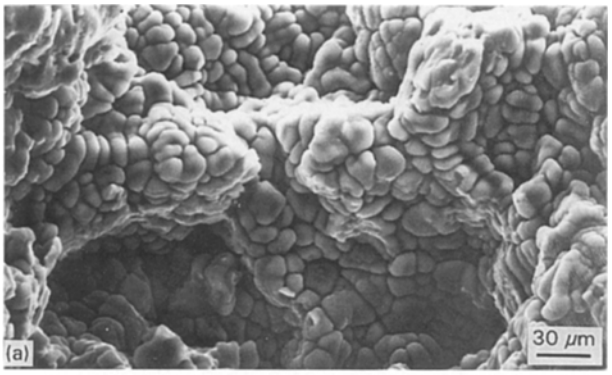

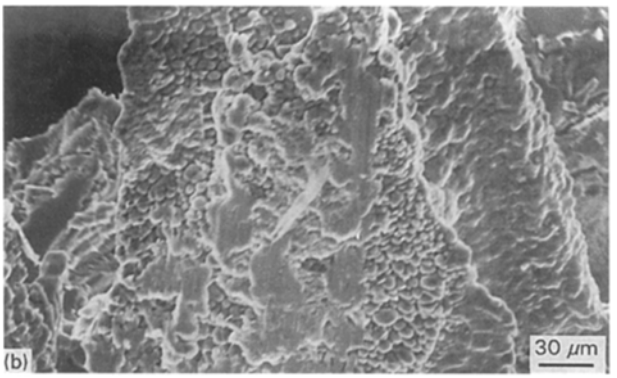

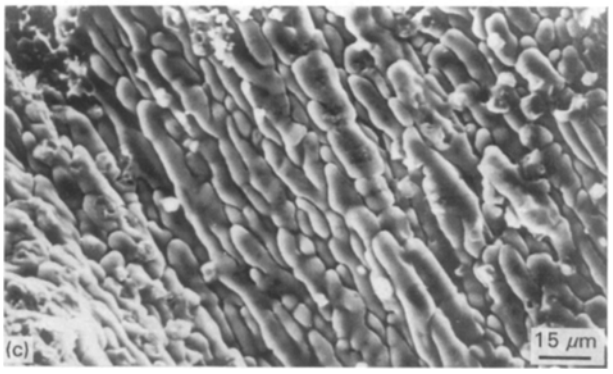

Figure 7 Fractography of solidification cracking for (a) Alloy 1, (b) Alloy 3, and (c) Alloy 4.

occurs in the mode of an intergranular and/or interdendritic cracking along the crack sensitive grain It is clearly observed that the solidification cracking occurs in the mode of an intergranular and/or interdendritic cracking along the crack sensitive grain boundaries. Fig. 6 shows the weld metal microstructure of alloy 1 which is observed to have a fine-equiaxed dendritic structure. Each grain has a substructure (marked as A) with the cell or dendrite array, and the intermetallic second phase constituents (marked as B) result from the solute redistribution during the solidification. It is well known that the more finely dispersed these intermetallic constituents are, the less deleterious is this influence on the solidification cracking susceptibility. Fig. 6 also shows the intermetallic constituents along the grain boundaries. As these intermetallic constituents are varied from a film-like product to a globular type product, the solidification cracking susceptibility of the weld metal is decreased.

The DSC curves for the alloys were analysed and the characteristics of the solidification temperature range (mush zone size) obtained from the melting and solidifying region of these curves are summarized in Table I as ΔT. From the results one may realize that alloy 1 shows the smallest solidification temperature range (ΔT) of 32.6 °C whereas alloys 4 and 5 have a larger value of 37–38 °C and alloy C shows the largest value of 40.2 °C. Comparing these values with the susceptibility to solidification cracking, it may be deduced that the larger the solidification temperature range, the higher the susceptibility to solidification cracking.

3.3. Fractography and EDAX analysis

Fig. 7(a–c) shows SEM fractographs of the interdendrite region of the laboratory alloys. They reveal features consisting of convex, round shaped protuberances and indicate the existence of a liquid film along the grain boundary at the moment of straining. The dominant characteristic features of these protuberances are (I) a dendritic type protuberance for alloy 1, (II) a flat type protuberance for alloy 3, and (III) a dendritic columnar type protuberance for alloy 4.

Alloy 1 in Fig. 7a has the primary and secondary arms of the dendrites, and the mode is almost globular thus creating the characteristic features of dendritic protuberance. In Fig. 7b of alloy 3, it is seen that the growth direction of the primary dendrites is parallel to the growth direction of the columnar grain, and the morphology of the secondary arms of the dendrites becomes indefinite, thus creating the characteristic flat protuberant appearance. In Fig. 7c, the primary dendrites and the growth direction of grains of alloy 4 can be still observed but the secondary arms of the dendrites could not be distinguished, and the surface of the primary arms of the dendrites become very smooth thus creating the characteristic features of the dendritic columnar appearance.

4. Discussion

The solidification cracking of a weld metal is known to be caused by the combination of mechanically and/or thermally induced strain, and a crack-susceptible microstructure. Since thermally induced strains are inherent in the process of melting and solidification, the only practical method of preventing solidification cracking lies in the elimination or control of the crack-susceptible microstructure. Welding parameters, solidification rates, alloy composition and microsegregation are factors which all play important roles in the control of the solidification cracking associated with welding.

It is generally considered that the solidification crack susceptibility of an alloy is strongly depended on the solidification temperature range or mushy zone size (ΔT) which was defined as the difference between the liquidus and solidus temperature during the solidification process. In general, the wider the solidification temperature range, the more the crack susceptibility for the solidification cracking of a weld metal. So far as

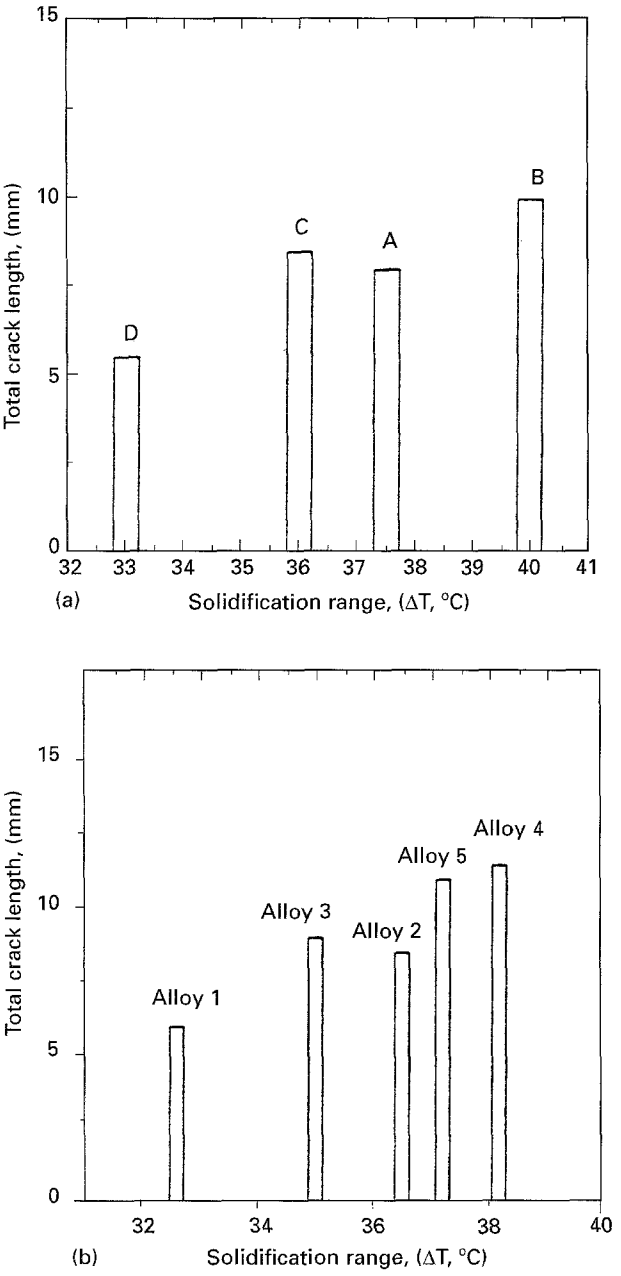

Figure 8 Total crack length versus solidification temperature range of the aluminum alloys; (a) commercial alloys and (b) laboratory alloys.

the solidification temperature range is concerned, the range is extended with increasing alloying content in aluminum alloys [14]. Therefore, from this point alone, it may be generally said that the solidification crack susceptibility increases with alloying element content.

The results of the Varestraint test and DSC analysis of the high strength aluminum alloy welds indicate that the solidification temperature range is affected more significantly by Cr than Mn and that the greater the solidification temperature range, the larger the total crack length and the greater the tendency for the solidification cracking. Fig. 8(a, b) shows this relationship for the commercial and laboratory alloys. In the fusion weld, the solidification is so rapid that the solute element(s) is/are not completely mixed, but exist in a compositional gradient extending into the liquid from the solid–liquid interface [15]. (Fig. 8).

Rapid solidification also gives rise to microsegregation of certain alloying elements and solute redistribution ahead of the moving solid–liquid interface. The degree of microsegregation is controlled primarily by the distribution coefficient, K, of the alloying element involved. In general, the more the value of K departs from 1.0, the greater will be the severity of the microsegregation.

Using the liquidus temperature variation equation, the degree of the solidification temperature range can be calculated by the difference between the liquidus temperature well ahead of the solid–liquid interface (T_L) and that at the solid–liquid interface (T_L^*) [16].

$$T_L = T_{mA} + M_L C_0 \quad (1)$$

where T_{mA} is the melting point of pure A(0% B) and M_L is the negative liquidus slope of a liquid whose composition is C_0. In an eutectic alloy of composition C_0, the temperature range over which solidification will occur would extend from the liquidus at C_0 to the eutectic temperature. The liquid at the solid–liquid interface has been enriched in solute elements and therefore has a lower liquidus temperature, T_L^*,

$$\begin{aligned} T_L &= T_{mA} + M_L(C_0/K - C_0) + M_L C_0 \\ &= T_{mA} + \frac{M_L C_0}{K} \end{aligned} \quad (2)$$

Since the solidification temperature range (ΔT) is the difference between T_L and T_L^*,

$$\begin{aligned} \Delta T &= T_{mA} + M_L C_0 - T_{mA} - \frac{M_L C_0}{K} \\ &= M_L C_0 \frac{(K-1)}{K} \end{aligned} \quad (3)$$

The $M_L(K-1)/K$ is defined as a relative potency factor (RPF) for the solidification cracking by Borland [16]. The larger the value of $M_L(K-1)/K$, the greater the solidification temperature range and the greater the tendency for solidification cracking. The results shown in Fig. 8 well coincide with Borlands explanation that the solidification cracking susceptibility increases with the mushy zone size (solidification temperature range) of the alloy.

Weld metal solidification cracking is found to be associated with the microsegregation produced at grain boundaries during the rapid solidification of the weld. Examination of the weld metal microstructure reveals that the intermetallic second phase constituents with globular shape are scattered along the grain boundaries. As the solidification cracking occurs in the grain boundary during the solidification stage, the amount and the shape of constituents in the grain boundary are the main metallurgical factors which seriously affect the solidification cracking susceptibility [17]. Since alloy 1 has the optimal contents of Mn as a Mn-dispersoid former and Zr as a grain refiner, compared with the other alloys [4] this alloy shows a grain boundary with fine globular particles rather than a film-like shape and exhibits high solidification cracking resistance. The weld metal microstructure also reveals that a cellular growth mode has occurred

in areas adjacent to the fusion line. Such a growth mode is supposed to be obtained from the steep temperature gradient which is present at the fusion line. The fractrographic examination in the fusion boundary of the high strength aluminum alloy weld (Fig. 7) reveals that the fracture surface morphologies (modes) change from the dendritic type protuberance for alloy 1 via a flat type protuberance for alloy 3 to a dendritic columnar type protuberance for alloy 4 with increasing solidification temperature range (mushy zone size). The zone size was obtained from the melting and solidifying region of the DSC curves and is summarized in Table 1 as the value of ΔT. The change in the fracture surface morphology is believed to result from the lowering of the solidification temperature of the molten grain boundary zone during the solidification process. The flat type fracture surface and the dendritic columnar type fracture surface show a relatively smooth columnar appearance, indicating these regions are associated with the ease of the solidification cracking propagation as compared to the dendritic type protuberance fracture surface with a curved and complex surface appearance. It also implies that the solidification cracking propagation of alloy 1, with a more dendritic protuberance type fracture surface feature, was arrested at high temperatures as compared to alloy 3 which has a flat type fracture surface or the alloys which have the dendritic columnar type fracture surface. Consequently, it is clear that a microstructure of finely dispersed intermetallic constituents with globular shape and a fracture surface of dendritic type protuberances is effective in reducing the solidification cracking susceptibility of high strength aluminum alloys.

5. Conclusion

The susceptibility to solidification cracking has been investigated for the 7000 series Al–Zn–Mg alloys by the Tig–a–Ma–Jig Varestraint test and the main conclusions are as follows.

(I) The solidification cracking susceptibility of Al–Zn–Mg alloys increases with the proportion of Cu and Cr alloying elements, and decreases with the proportion of Mn and Zr alloying elements.

(II) The optimum amounts of added Mn and Zr in order to reduce the solidification cracking susceptibility are found to be 0.68–0.72% and 0.12–0.16%, respectively.

(III) Mn is very effective in reducing the total crack length and thus improving the resistivity to solidification cracking in Al–Zn–Mg alloy welds.

(IV) The mushy zone size (ΔT) during the solidification of the weld metal increases as the Cr content increased in these alloys.

(V) The fracture surface mode of the solidification cracks under the optimum amount of Mn are dendritic type protuberances for the alloy with a low Zr content and no Cr content flat type protuberances for an alloy with a high Zr content and low Cr content and dendritic columnar type protuberances for an alloy with high Zr content and high Cr content respectively.

References

1. H. WESTENGEN, L. AURAN and O. REISO, *Aluminum* **57** (1981) 797.
2. R. E. SANDERS, Jr. and E. A. STRAKE, Jr., *Mater. Sci. Eng.* **28** (1977) 53.
3. J. S. SANTNER, *Metall. Trans.* **9A** (1978) 769.
4. D. S. PARK and S. W. NAM, *Metall. Trans. A (Comm.)* **25** (1994) 1547.
5. S. W. NAM, Development of Weldable High Strength Aluminum Alloy(II), KAIST Report, August, 1994, p. 8.
6. R. SANDSTROM, in Proceedings of the 5th International Conference on Aluminum Weldments, Aluminum-Verlag, Dusseldorf, Munich, April 1992, p. 531.
7. F. MATSUDA, *Trans. of Japan Welding Research Institute* **14** (1985) 99.
8. K. NAKATA, *J. of the Japan Welding Society* **4** (1986) 115.
9. M. J. DVVORNAK and D. L. OLSON, *Welding Journal* **70** (1993) 271S.
10. T. FUKUI, *J. of the JWS* **35** (1966) 1122.
11. S. W. NAM and D. S. PARK, High Strength Aluminum Alloy with Good Weldability, U. K. Patent No. GB2246578B, Mar. 1, 1995.
12. C. D. LUNDIN, in Proceedings of the 2nd International Conference on Recent Trend in Welding Science and Technology, ASM Tennessee, May 1989, p. 699.
13. F. MATSUDA, *Trans. of JWRI* **14** 2 (1985) 101.
14. Q. Z. DIAO, *Metall. Trans.* **24A** (1993) 963.
15. S. KOU, *Welding Research Council Bulletin* **320** (1986) 6.
16. J. C. BORLAND, *Treatise on Material Science and Technology*, Academic Press 1989, 555.
17. K. NAKATA, in Proceedings of the 6th International Conference on Aluminum Weldments, Cleveland, April 1995, p. 387.

Received 13 June 1995
and accepted 20 November 1995